HAWC2 course

Lesson 3a: Aerodynamic modeling and implementation in HAWC2

Helge Aagaard Madsen
Leonardo Bergami

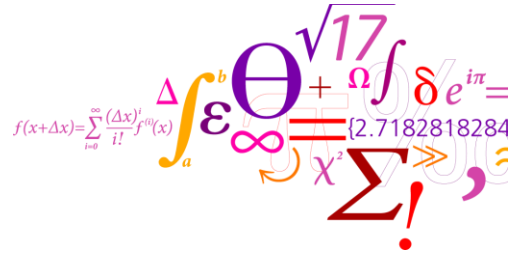

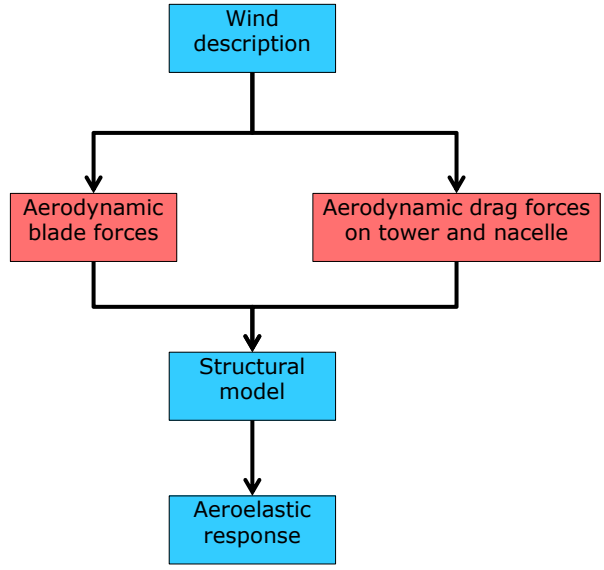

Overview of aerodynamic force calculation

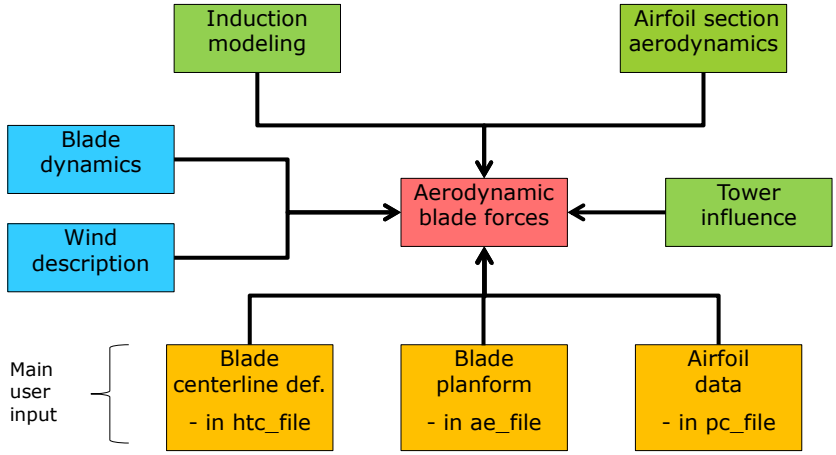

Airfoil section aerodynamics

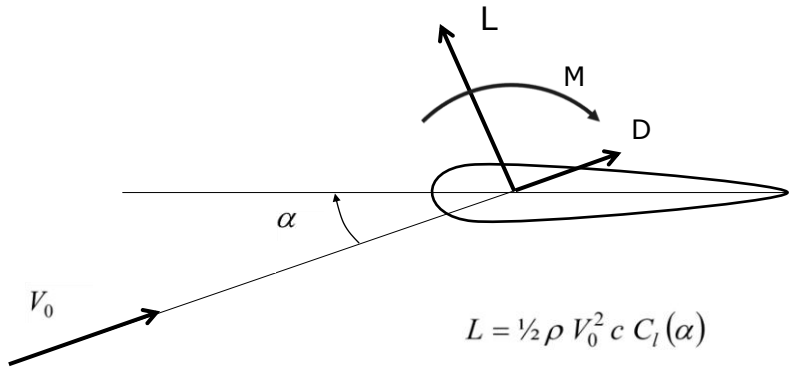

$$L = \tfrac{1}{2}\rho V_0^2 c C_l(\alpha)$$

$$D = \tfrac{1}{2}\rho V_0^2 c C_d(\alpha)$$

$$M = \tfrac{1}{2}\rho V_0^2 c C_m(\alpha)$$

Steady airfoil data and unsteady effects

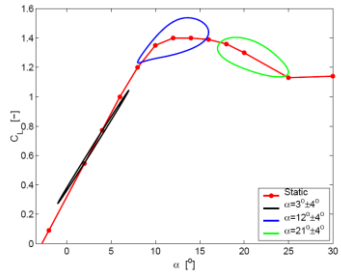

Steady C_l, C_D *and* C_m data from pc_file

Modeling of unsteady effects to be shown by **Leonardo** later

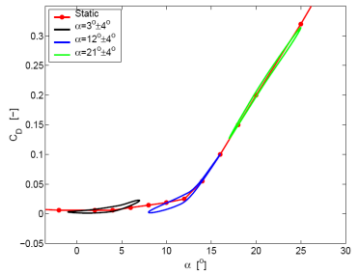

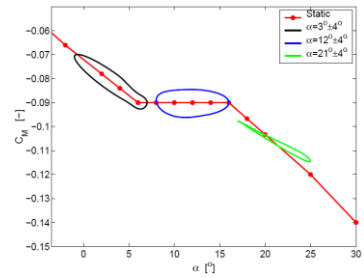

Induction modelling

Increasing model complexity

- BEM Actuator disc
- CFD Actuator disc
- Fixed wake vortex codes
- Free wake vortex codes
- CFD Actuator line
- Full 3D CFD

Airfoil data

Actuator disc ⇒ Model of ideal turbine - Infinitely many blades

The reaction of the blade forces applied on the flow as volume or body forces

BEM equations (relation between induction and load) derived for a constant loaded actuator disc

The energy conversion – Bernoulli

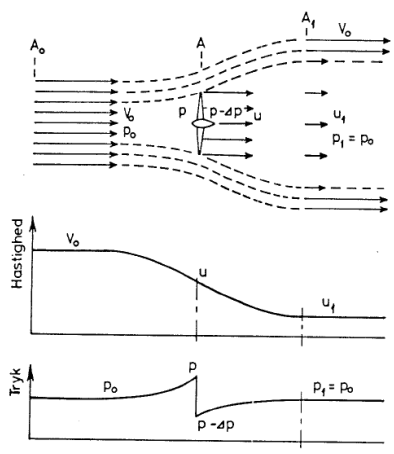

$$T = \Delta p A$$

Bernoulli

$$\tfrac{1}{2}\rho V^2 + p = H$$

Applied before and after rotor disc

$$p_0 + \tfrac{1}{2}\rho V_0^2 = p + \tfrac{1}{2}\rho u^2$$

$$p - \Delta p + \tfrac{1}{2}\rho u^2 = p_0 + \tfrac{1}{2}\rho u_1^2$$

$$\Rightarrow \Delta p = \tfrac{1}{2}\rho\left(V_0^2 - u_1^2\right)$$

The energy conversion – 1D momentum

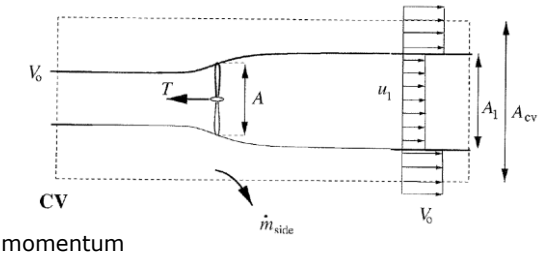

Change in momentum

$$\vec{T} = \dot{m}\Delta\vec{V} \qquad \Rightarrow T = \rho V_0 A_{CV} V_0 - \rho u_1 A_1 u_1 - \rho V_0 (A_{CV} - A_1) V_0 - \dot{m}_{side} V_0$$

Conservation of mass and insert in momentum equation

$$\rho A_{CV} V_0 = \rho A_1 u_1 + \rho (A_{CV} - A_1) V_0 + \dot{m}_{side} \qquad \Rightarrow \dot{m}_{side} = \rho A_1 (V_0 - u_1)$$

$\dot{m} = \rho u A = \rho u_1 A_1$ yields $T = \dot{m}(V_0 - u_1)$

Combining momentum and Bernoulli

$$u = \tfrac{1}{2}(V_0 - u_1)$$

1D momentum continued

Introducing the induction factor a

$$u = (1-a)V_0 \qquad u_1 = (1-2a)V_0$$

Extracted power for an ideal rotor is difference in power from inlet to outlet

$$P = \tfrac{1}{2}\dot{m}\left(V_0^2 - u_1^2\right)$$

$$C_p = \frac{P}{P_{avail}} = \frac{2\rho A V_0^3 a(1-a)^2}{\frac{1}{2}\rho V_0^3 A} = 4a(1-a)^2$$

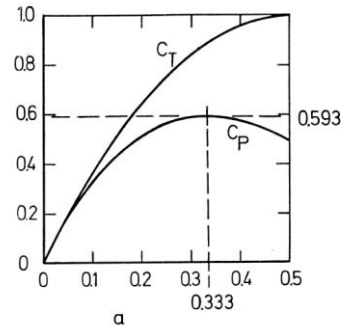

Similar for the torque

$$T = \rho u A (V_0 - u_1)$$

$$C_T = \frac{T}{T_{avail}} = \frac{2\rho A V_0^2 a(1-a)}{\frac{1}{2}\rho V_0^2 A} = 4a(1-a)$$

The relation between thrust and axial induction

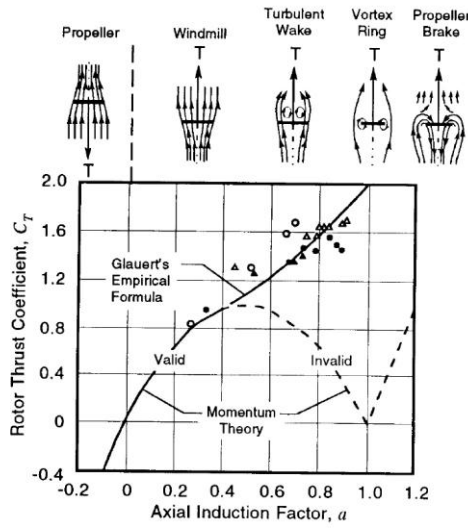

$$u = (1-a)V_0$$
$$C_T = 4a(1-a)$$
$$C_T = \frac{T}{\frac{1}{2}\rho V_0^2 A}$$

⇩

Afterwards this equation is used locally in a point

Blade Element Momentum theory

Rotor plane is discretized into

independent concentric annular elements and azimuthal variation of loading

on which the 1D assumption is applied

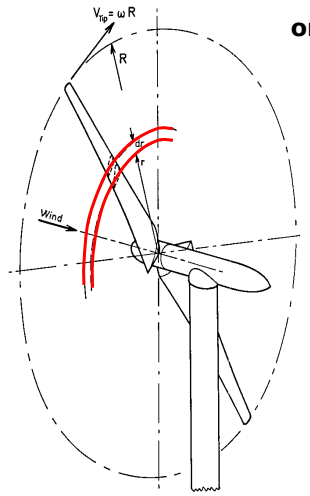

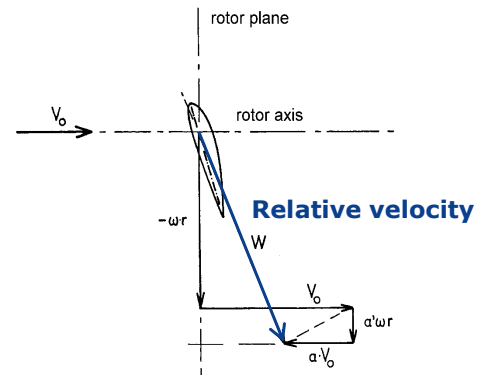

Induction model in HAWC2

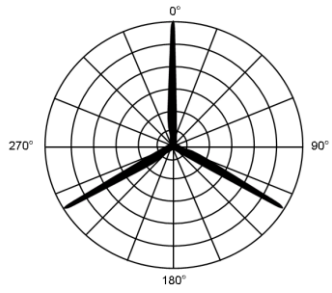

A non-rotating grid is defined in which induced velocities are calculated. Enables modelling of azimuthal variation of induction e.g. **due to shear** in inflow or **due to turbulence**

BEM in HAWC2 formulated locally in grid.

$$Blade\ element\ theory: \quad dT = \frac{1}{2}\rho W^2 C_y(\alpha) c N_B$$

Axial thrust at given radial station on the blade

$$CT = \frac{dT}{\frac{1}{2}\rho V_\infty^2 2\pi R} \Rightarrow$$

The local thrust coefficient is found

$$CT = \frac{W^2 C_y(\alpha) c N_B}{2\pi r V_\infty^2}$$

V_∞ is the magnitude of the local free wind speed.

$$a \equiv -\frac{u_{induc,axial,local}}{|V_{\infty,local}|}$$

$C_y(\alpha)$ and $C_x(\alpha)$ are projections of $C_l(\alpha)$ and $C_D(\alpha)$ perpendicular and tangential to rotor plane, respectively

BEM in HAWC2 continued

Momentum theory: $CT = 4a(1-a)$

for $a > 0.33$ *the Glauert empirical correlation between a and CT is used*

The solution to the above equation is written on the form:

$$a = k_3 CT^3 + k_2 CT^2 + k_1 CT + k_0$$

However, the $a = f(CT)$ *relation can alternatively be derived from an actuator disc computation on the rotor and would then be a function of position on the rotor disc*

k(3)=0.0892074

k(2)=0.0544955

k(1)=0.251163

k(0)=-0.0017077

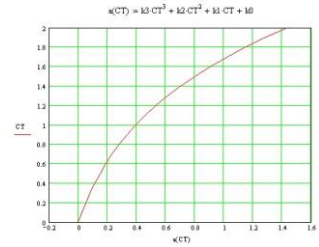

Tangential wake rotation

Angular momentum on annular ring

$$dQ = \rho(2\pi r\, dr)(1-a)V_\infty(2a'\Omega)$$

Tangential blade forces on annular ring

$$dQ = \tfrac{1}{2}\rho W^2 C_x(\alpha)cN_B r\, dr$$

Above equations solved for the tangential induction factor

$$a' = \frac{W^2 C_x(\alpha)cN_B}{8\pi r^2(1-a)V_\infty\Omega}$$

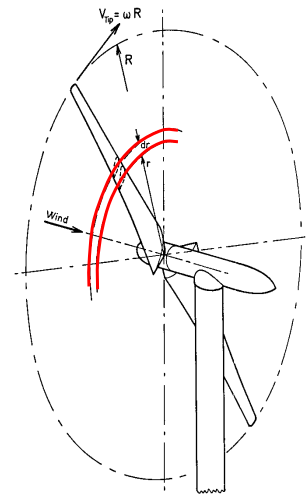

Sub models to the induction modeling

- **tip correction model** to account for a finite number of blades
- a **yaw model** to account for skew inflow
- a **dynamic induction model** to account for time lag in update of wake due to load changes

Tip loss correction model in HAWC2

The Prandtl tip correction – take into account finite number of blades – radial velocity at the blade tip

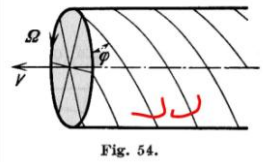

Fig. 54.

This is a suitable form according to the general theory of flow in terms of the complex variable, it has the correct periodicity, and it gives zero normal velocity on the surface of the lines. The general type of flow is as shown in Fig. 60. Between the lines, far from the edges, the fluid is at rest, but near the edges there is a small upward flow.

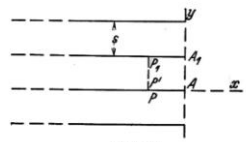

Fig. 59.

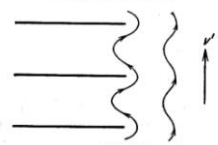

Tip loss correction model in HAWC2

- The tiploss model used in HAWC2 is based on the modified expression by Wilson and Lissaman

$$F = \frac{2}{\pi}\cos^{-1}\left(\exp\left(-\frac{N_B}{2}\frac{(1-r/R)}{(r/R)\sin\phi}\right)\right)$$

- This factor is inserted in the induction calculation

$$CT = 4a\ F(1-a) \quad or \quad \frac{CT}{F} = 4a(1-a)$$

$$CT^* = \frac{CT}{F}$$

$$a = k_3\,CT^{*3} + k_2\,CT^{*2} + k_1\,CT^*$$

Yaw correction model in HAWC2

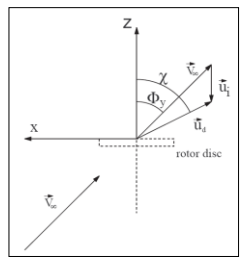

Based on model by Glauert

$$T = A\rho\left|\vec{V}_\infty + \vec{u}_i\right|2u_i$$

$$CT = 4a\left(1 + a^2 - 2a\cos\Phi_y\right)^{1/2}$$

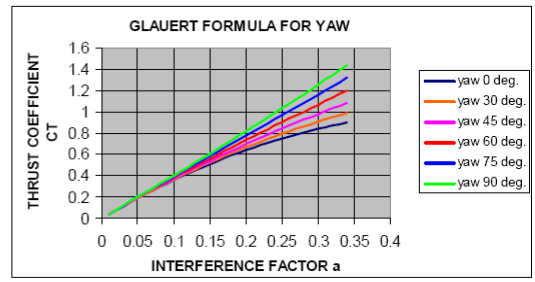

Azimuthal impact on yawed inflow

$$u_{ix} = u_i\left(1 + k_x\, r\cos(\psi) + k_y\, r\sin(\psi)\right)$$

Ψ Is the azimuth angle

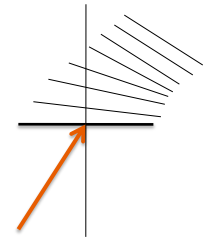

Table 3.1. *Various Estimated Values of First Harmonic Inflow*

Author(s)	k_x	k_y
Coleman et al. (1945)	$\tan(\chi/2)$	0
Drees (1949)	$(4/3)(1-\cos\chi-1.8\mu^2)/\sin\chi$	-2μ
Payne (1959)	$(4/3)(\mu/\lambda/(1.2+\mu/\lambda))$	0
White & Blake (1979)	$\sqrt{2}\sin\chi$	0
Pitt & Peters (1981)	$(15\pi/23)\tan(\chi/2)$	0
Howlett (1981)	$\sin^2\chi$	0

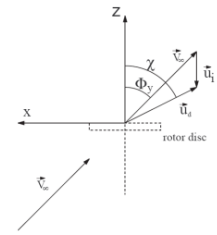

In HAWC2 the Coleman method is used with a constant of 0.4 instead of 0.5

$$\tan(\chi) = \frac{V_\infty \sin(\Phi_y)}{V_\infty \cos(\Phi_y - u_i)}$$

Yawed inflow

The reduction K_a of the induction factor a as function of yaw angle and thrust coefficient wass shown in the figure above and in order to use the correction directly in the induction calculation the following polynomial fit has been derived:

$$K_a = CT^3 k_3 + CT^2 k_2 + CT\, k_1$$

where the parameters k_3, k_2 and k_1 depends on the yaw angle (radians) in the following way:

$$k_3 = -0.6481\Phi_y{}^3 + 2.1667\Phi_y{}^2 - 2.0705\Phi_y$$

$$k_2 = 0.8646\Phi_y{}^3 - 2.6145\Phi_y{}^2 + 2.1735\Phi_y$$

$$k_1 = -0.164\Phi_y{}^3 + 0.4438\Phi_y{}^2 - 0.5136\Phi_y$$

Modification of induction

$$a_{cor} = K_a a$$

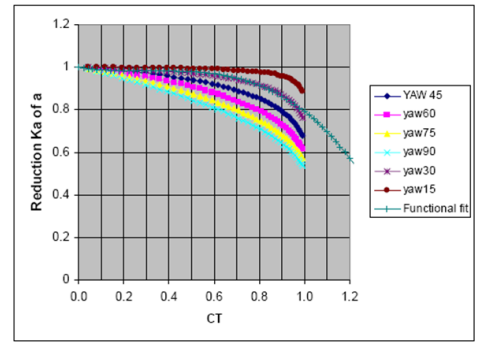

Comparison between HAWC2 and CFD actuator disc computations

30deg

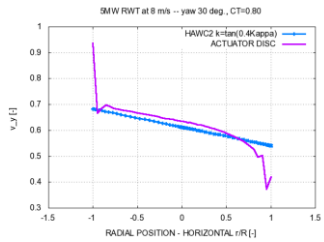

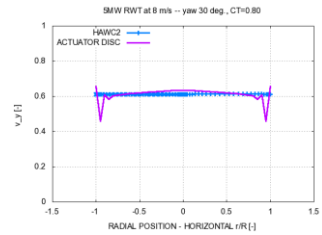

60deg

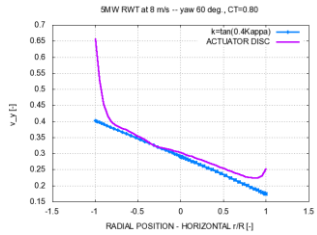

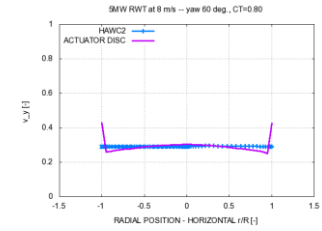

Dynamic inflow model in HAWC2

Effect of dynamic inflow – numerical actuator disc simulations – step change in loading

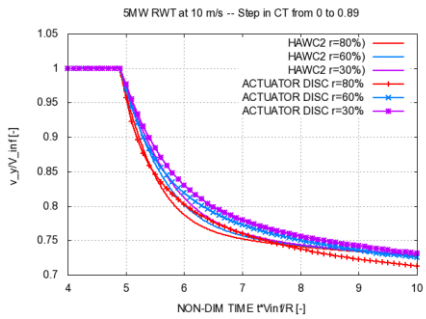

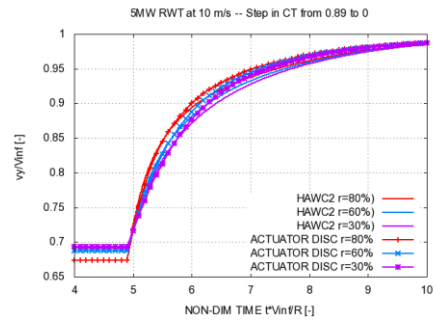

Effect of dynamic inflow – numerical actuator disc simulations – step change in loading

$$\tilde{\tau} = \tau \frac{V_\infty (1 - 1.5a)}{R}.$$

In both the BEM and the NW model, this is the approach used, and as will be seen later in the paper, this assures that the time constants reflects the slower development of the wake when high induction are present. The effect of changing the normalization can be seen in Figure 1, where the use of the actual wake velocity makes the curves collapse.

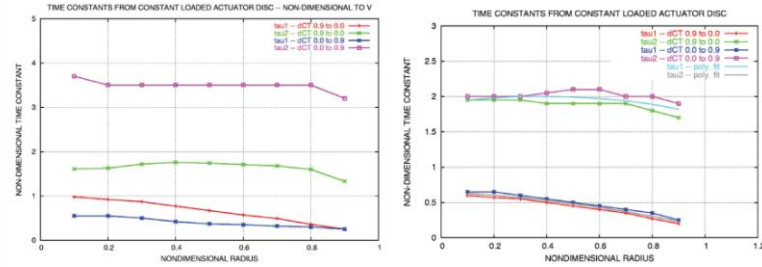

Figure 1: The dependency of the non-dimensionale time constant on the choice of normalization velocity used, left figure using the free stream velocity, right figure shows the use of the actual wake velocity.

Dynamic inflow

$$\tau^*_{NW}\left(r/R\right) = k_2\left(r/R\right)^2 + k_1\left(r/R\right)^1 + k_0$$

	NW	*FW*
k2	-0.4783	-0.4751
k1	0.1025	0.4101
k0	0.6125	1.9210

Dynamic inflow model in HAWC2

The Dynamic indflow ins handled by two first order filters coupled in parallel with weight factors

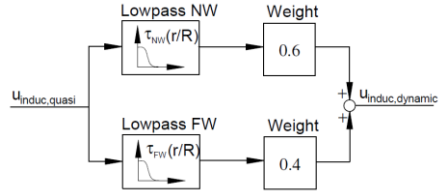

$$\tau_{FW}\left(r/R\right) = \tau^*_{FW}\left(r/R\right)\frac{R}{V_{\infty,y}\,\mathrm{MAX}\left[1+3\frac{V_{induc,y}}{V_{\infty,y}},0.2\right]}$$

$$\tau_{NW}\left(r/R\right) = \tau^*_{NW}\left(r/R\right)\frac{1.8R}{V_{\infty,y}\,\mathrm{MIN}\left[1-3\frac{V_{induc,y}}{V_{\infty,y}},2.0\right]}$$

The non-dim time constants was found to approximately 2.0 for the far wake contribution and 0.5 for the near wake part

BEM procedure

- For each point in the polar grid
  1. Get the local wsp and use local induced wsp from previous timestep/iteration
  2. Get the local CT calculated at the two neighboring blades if the local wsp and induction was used there.
  3. Account for Prandtl tiploss
  4. Interpolate CT based on azimuthal distance between grid point and the two blades. Now the local CT is known.
  5. Calculate local induction factor a
  6. Correct mean level of a based on skew inflow angle.
  7. Calculate tangential induction factor a_m
  8. Calculate induced wind speeds axial (1) and tangential
  9. Correct for azimuthal variations of axial induction u related to skew inflow angle incl. axial induction influence..
  10. Update u and u_t in time based on two first order low pass filters. One for near wake contribution and one for far wake.

- For each point on the blade
  11. Get the induced velocity based on azimuthal interpolation of the two closest grid points at same radius.

Induction model in HAWC2

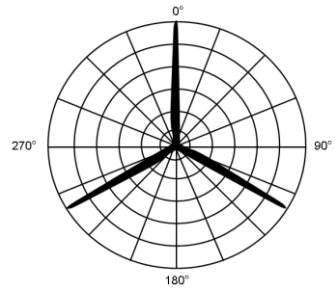

A non-rotating grid is defined in which induced velocities are calculated. Enables modelling of azimuthal variation of induction e.g. due to shear in inflow or due to turbulence

Validation results

Comparison

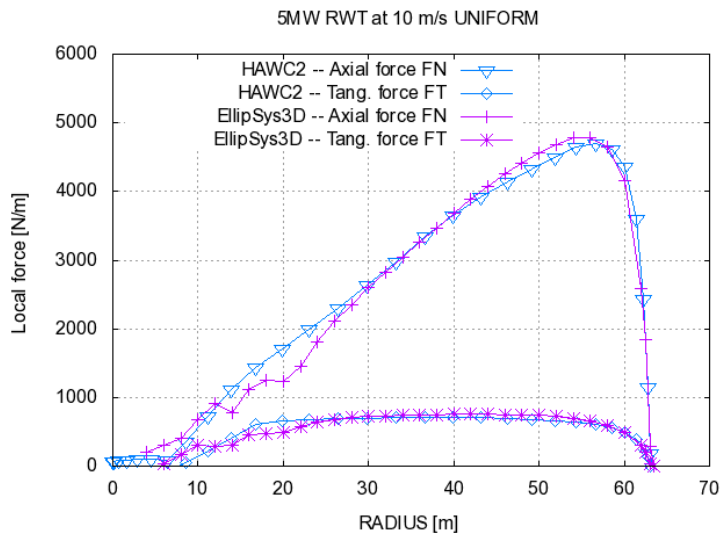

Special shear (1)

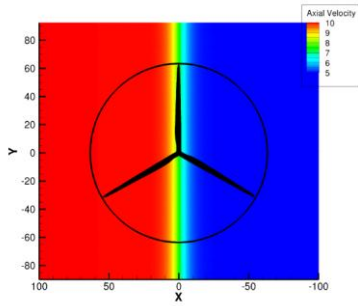

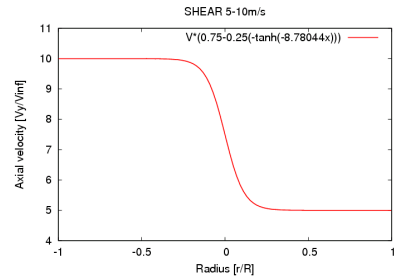

Special shear (2)

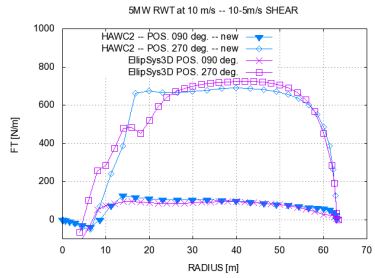

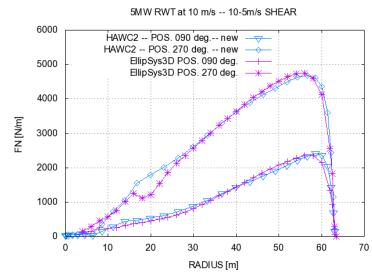

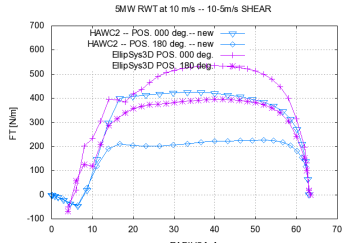

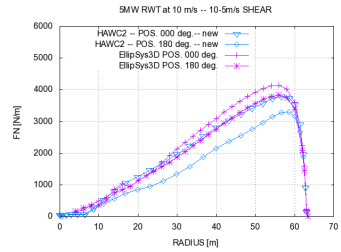

Special shear (3)

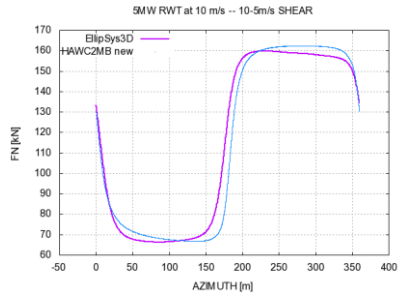

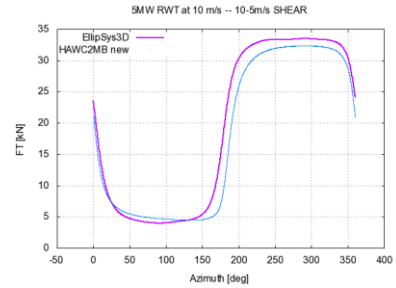

Wake situation

270°

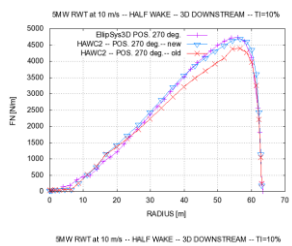

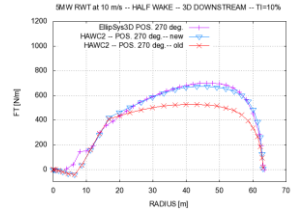

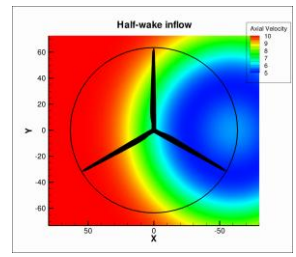

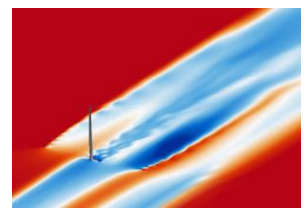

90°

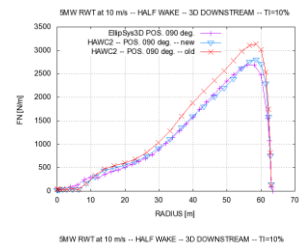

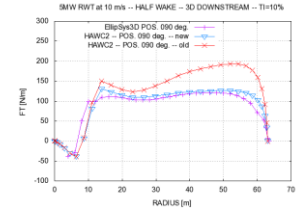

Examples of limitations of the BEM model

All rotors with the same uniform loading, CT=0.89

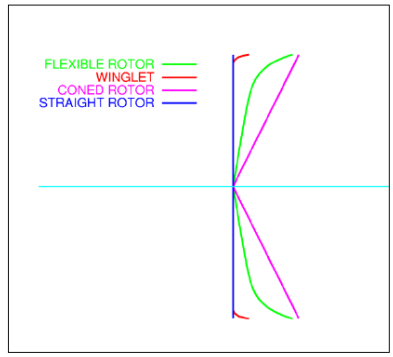

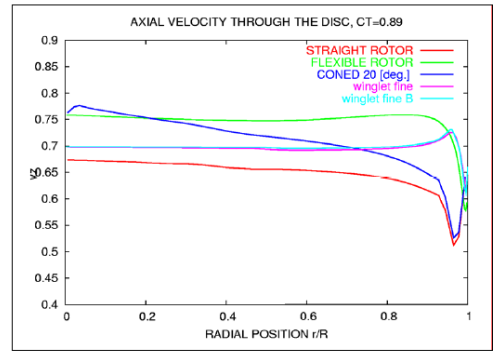

For such special rotors a user defined a-CT relation can be used if the characteristic is known from e.g. CFD actuator disc simulations

Tower influence modelling in HAWC2

- models for both an upstream and a downstream position of the rotor is implemented

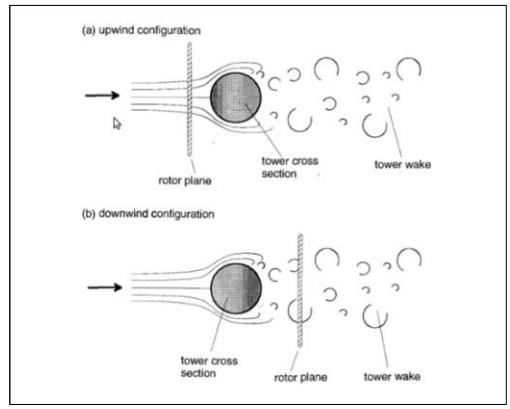

Tower influence modelling - upstream

Flow model based on the potential flow solution around a cylinder

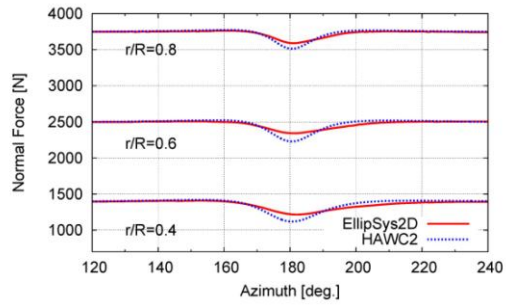

Figure 23. Comparison of HAWC2 and EllipSys2D normal force coefficients as function of blade azimuth for the upwind configuration of the UPWIND turbine at the three radial sections.

Tower influence modelling - downstreamam

Flow model based on the boundary solution for a jet into a flow at rest

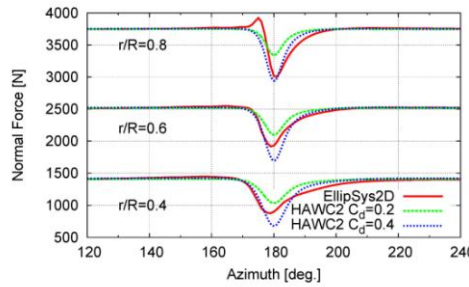

Figure 24. Comparison of HAWC2 and EllipSys2D normal force coefficients as function of blade azimuth for the downwind configuration of the UPWIND turbine at the three radial sections.

Tower influence modelling - downstream

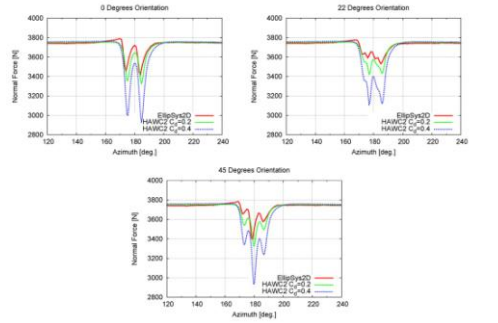

Figure 25. Comparison of HAWC2 and EllipSys2D normal force coefficients as function of blade azimuth for the four leg tower configuration for the three tower orientations.

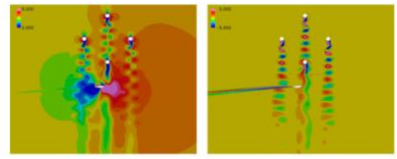

Figure 22. Snapshot of axial velocity and vorticity for the four leg configuration for the 80% radius blade section at 45 degrees orientation to the tower.

Thank you for
your attention